Title:

Renal tumours in a *Tsc2*^{+/-} mouse model do not show feedback inhibition of Akt and are

effectively prevented by rapamycin

Authors and affiliations:

Jian Yang[1], Maria Kalogerou[1], Paulina A. Samsel[1], Yadan Zhang[1], David F. R. Griffiths[2],
John Gallacher[3], Julian R. Sampson[1] and Ming Hong Shen[1]

[1]Institute of Medical Genetics and [2]Section of Pathology, Institute of Cancer and Genetics,
School of Medicine, Cardiff University, Heath Park, Cardiff CF14 4XN, UK

[3]Department of Primary Care & Public Health, School of Medicine, Cardiff University,
Heath Park, Cardiff CF14 4YS, UK

Running Title: Akt/mTOR signalling and renal tumour prevention

Corresponding authors:

Ming Hong Shen (To communicate with the Editorial and Production Offices.)

Telephone: +44 (0)29 20683649   Fax: +44(0)2920746551   Email: shenmh@cf.ac.uk

or

Julian R Sampson

Telephone: +44 (0)29 20744050   Fax: +44(0)2920746551   Email: Sampson@cf.ac.uk

Word count: 4318

ABSTRACT

Tuberous sclerosis (TSC) is an inherited syndrome in which tumours in multiple organs are characterised by activation of mammalian target of rapamycin complex 1 (mTORC1). Previous work suggests that mTORC1 activation is associated with feedback inhibition of Akt, a substrate of mammalian target of rapamycin complex 2 (mTORC2). This could limit TSC-associated tumour growth but lead to paradoxical promotion of tumour cell survival upon treatment with mTOR inhibitors. However, Akt/mTOR signalling has not been fully investigated in TSC-associated tumours and it has been uncertain whether mTOR inhibition can prevent TSC-associated renal tumourigenesis. In this study, we investigated Akt/mTOR signalling in renal tumours using a $Tsc2^{+/-}$ mouse model and tested whether mTOR inhibition could prevent renal tumourigenesis. We found that all renal lesions including cysts, adenomas and carcinomas exhibited activation of both Akt and mTORC1 as evidenced by increased protein expression and phosphorylation of Akt and mTOR and their downstream targets. PKCα was also highly expressed and phosphorylated in these lesions, consistent with activation of mTORC2. Surprisingly, IRS proteins were highly expressed, in contrast to a striking decrease seen in cultured $Tsc2^{-/-}$ mouse embryonic fibroblasts, suggesting one mechanism through which loss of feedback inhibition of Akt may occur in mTORC1 hyperactivated Tsc-associated tumours. Long term treatment with rapamycin reduced both Akt and mTORC1 activity in normal kidney tissues and blocked the development of all types of renal lesions. In conclusion, in contrast to previous studies, we found that Akt signalling is not inhibited in Tsc-associated renal lesions and that by partially inhibiting the Akt/mTOR pathway, rapamycin is highly effective in preventing Tsc-associated tumours.

Key words: Tuberous sclerosis, renal tumours, Akt, mTOR, rapamycin

INTRODUCTION

The Akt kinase family integrates many cell signals, modulates multiple cellular activities and has a large number of molecular targets and effectors (1). The serine/threonine kinase mTOR is associated with two distinct multi-protein complexes (mTORC1 and mTORC2) and acts downstream of PI3K/Akt to regulate cellular processes such as metabolism, growth, proliferation, survival, differentiation, self-renewal, autophagy and apoptosis (2-4). Many components of the PI3K/AKT/mTOR signalling pathway are mutated in human cancers (5-7). Several upstream negative regulators of mTOR are tumour suppressors and are mutated in inherited tumour syndromes including tuberous sclerosis (TSC) (8-13). TSC is caused by mutations of *TSC1* or *TSC2* and characterised by development of tumours in many organs. Kidney tumours termed angiomyolipomas (AMLs) are among its most frequent manifestations and lead to significant morbidity and mortality due to haemorrhage and kidney failure. The TSC1 and TSC2 proteins form a complex that down-regulates mTOR activity and TSC-associated tumours show aberrant activation of mTOR signalling in both patients and animal models.

In mouse embryonic fibroblasts (MEF) lacking *Tsc1* or *Tsc2*, Akt signalling is inhibited by a negative feedback loop (14, 15). In these cells, mTOR activates p70 S6 kinase (S6K) that inhibits Akt activity by direct phosphorylation of IRS1 and by repressing IRS1 gene expression (16). IRS2 is also down-regulated by mTOR activation (16, 17). More recently, Grb10, the growth factor receptor–bound protein 10, has been identified as a substrate of mTORC1 that also negatively regulates PI3K/Akt activity in *Tsc1* or *Tsc2* null MEF cells (18, 19). These cells have reduced tumorigenic potential while myr-Akt–expressing $Tsc2^{-/-}$ MEF cells demonstrate accelerated tumour growth in nude mice (20). Feedback inhibition of Akt signalling has been reported to limit the growth of tumours in the liver of a $Tsc2^{+/-}$ mouse model (21). These results suggest that feedback inhibition of Akt signaling in cells with no

3

functional TSC1 or TSC2 might contribute to the low malignant potential of tumours in TSC patients. In contrast to the usually benign features of renal AMLs in human TSC, $Tsc1^{+/-}$ or $Tsc2^{+/-}$ mice develop frequent renal cell carcinomas (22, 23). It remains to be fully assessed whether negative feedback on Akt signalling occurs in these tumours.

The mTOR inhibitor rapamycin and its analogues (rapalogs) have been used to treat a variety of human cancers as well as patients with TSC. TSC-associated tumours including AMLs and subependymal giant cell astrocytomas (SEGA) exhibit consistent but partial and reversible responses to rapamycin and the rapalog everolimus (24-27). As yet, no properly designed studies have investigated whether these drugs can prevent tumourigenesis in TSC patients or animal models.

In this study, we examined Akt/mTOR signalling in renal lesions and corresponding normal kidney tissues using a $Tsc2^{+/-}$ mouse model. We also tested the efficacy of rapamycin for prevention of renal tumours and its effect on Akt/mTOR signalling. In contrast to previous studies, we found that feedback inhibition of Akt signalling was not seen in renal lesions of $Tsc2^{+/-}$ mice. We also found that rapamycin was highly effective in preventing tumour development.

RESULTS

Renal Lesions in $Tsc2^{+/-}$ mice show loss of Tsc2 and hyperactivation of mTORC1 signalling

Histology and immunohistochemistry (IHC) were used to analyse spontaneously arising renal lesions in both kidneys of 15 $Tsc2^{+/-}$ mice at the age of 10 months. These lesions included microscopic dysplastic lesions (renal intraepithelial neoplasias or RINs), cysts, papillary and solid adenomas, and carcinomas (Supplemental Figure 1), and were highly proliferative

(Supplemental Figure 2). By IHC, we found that 91.1 % (123/135) of renal lesions had no detectable Tsc2, 8.2 % (11/135) had markedly reduced expression and only one cyst out of 135 lesions had an increased expression of Tsc2 compared to neighbouring kidney tissues (Figure 1; Supplemental Table 1). By PCR, loss of heterozygocity (LOH) of *Tsc2* was observed in 3 of 4 renal tumours tested (Figures 2c and 3c). By Western blot, little Tsc2 expression was detected in tumours with LOH (Figures 2c and 3c). No LOH was detected in tumour 4 but Tsc2 expression was substantially reduced, suggesting an alternative mechanism affecting the wild type allele such as an intragenic mutation or epigenetic suppression (Figures 2c and 3c).

As expected, increased protein levels of mTOR and its downstream signalling components S6K and S6 ribosomal protein (S6) were observed in all renal lesions (Figure 2a, b and c). Hyper-activation of mTOR was evidenced by increased phosphorylation of mTOR at S2448 and S2481 as well as increased phosphorylation of its major effectors S6K at T389, S6 at S235/236, and 4EBP1 at T37/46, S65 and T70 (Figure 2a, b and c, Supplemental Figure 3). These results indicated that in the majority of renal tumours of *Tsc2*^{+/-} mice Tsc2 was lost leading to aberrant activation of mTOR/S6K signalling.

Akt activity is not inhibited in renal lesions of *Tsc2*^{+/-} mice

We re-examined the previously reported suppression of Akt signalling in cultured *Tsc1* or *Tsc2* deficient cells (Supplemental Figure 4). As expected, immortalised *TP53*^{-/-}*Tsc2*^{-/-} MEF cells showed mTOR activation but reduced Akt activity compared to control *TP53*^{-/-}*Tsc2*^{+/+} MEF cells. Similarly, though less pronounced, changes were seen in non-immortalised *Tsc1*^{-/-} MEF cells (Supplemental Figure 4).

We then used IHC and Western blot to investigate Akt signalling in renal lesions of *Tsc2*^{+/-} mice. All lesions showed an increased level of total Akt compared to adjacent normal kidney

tissues (Figure 3a and c). Levels of Akt1, Akt2 and Akt3 were all increased in tumours (Figure 3c). Since Akt is fully activated by phosphorylation of the activation loop at T308 and the hydrophobic motif at S473, and stabilised by phosphorylation of the turn motif at T450, we then examined the phosphorylation levels at these sites. In contrast to the findings in cultured MEFs, elevated phosphorylation of Akt at S473 and at T450 as well as Akt1 at S473 was evident in all lesions (Figures 3a, c and Supplemental Figure 3). Phosphorylation of Akt at T308 was also present in a proportion of tumour cells in renal lesions (Figure 3a and c). Expression of the Akt targets HIF1α and GLUT1 was increased, and increased phosphorylation of an array of well characterised Akt substrates was observed including eNOS, MDM2, GSK3α, GSK3β, IKKα, RAF1and FOXO1A (Figure 3b and c; Supplemental Figures 3 and 5). Of note, higher expression of both β-actin and GAPDH was observed in tumour cells than adjacent normal kidney tissues (Supplemental Figure 6). Therefore, relative protein and phosphorylation levels of Akt/mTOR signalling components in tumour samples might be underestimated on Western blot analysis.

mTORC2 specifically phosphorylates the hydrophobic motif and turn motif sites of Akt at S473 and T450 (28, 29). We therefore speculated that other mTORC2 substrates such as PKCα, another AGC kinase family member, may also be highly phosphorylated at similar sites in Tsc-associated tumours. We examined the expression and phosphorylation of PKCα in renal lesions of $Tsc2^{+/-}$ mice by IHC and Western blot. All renal lesions examined had increased expression and phosphorylation of PKCα at T638 and S657 (Figure 4).

mTOR also negatively regulates PI3K/Akt by reducing expression of PDGFRs (20). We found that PDGFRβ expression was reduced in renal lesions but expression and phosphorylation of Erk1/2, another downstream target of PDGFRs, were increased, indicating activation of the MAPK pathway, again in contrast to $Tsc2$ null MEFs (Figure 5, Supplemental Figure 7). These data demonstrate that Akt, PKCα and the MAPK pathway are

not inhibited in renal lesions of *Tsc2*^{+/-} mice despite hyper-activation of mTOR/S6K signalling.

IRS protein levels are increased in renal tumours of *Tsc2*^{+/-} mice

To investigate the mechanisms through which negative feedback inhibition of Akt is lost in Tsc-associated renal tumours, we used Western blot, IHC and quantitative real time PCR (q-PCR) to assess components of the feedback loop. We found that expression of both insulin receptor (IR) and IGF1 receptor (IGF1R) was reduced in renal tumours (Figure 5 and 6). Phosphorylation of IGF1R at Y1135/1136 (IR at Y1150/1151) was also reduced (Figure 5). Similar findings were obtained from *Tsc2* null MEFs (Figure 5). However, unlike *Tsc2* null MEFs, tumours had increased levels of IRS proteins and slightly reduced expression of Grb10 protein (Figures 5 and 6). Phosphorylation of numerous serine residues of these proteins is regulated by mTOR and sensitive to rapamycin (supplementary Figure 8). In both renal tumours and MEFs, IRS, IRS2 and Grb10 were highly phosphorylated at S302, S731and S476 respectively (Figures 5 and 6). However, very little phosphorylation at S501/503 was detected by Western blot in normal kidneys or renal tumours (Figures 5), and only slightly increased phosphorylation at these sites was detected by IHC in these tumours (Supplemental Figure 9). Finally, transcription of *IGF1R*, *IRS1* and *IRS2* was suppressed in renal tumours although to a less extent as observed in *Tsc2* null MEFs (Supplemental 10). These findings suggest that increased levels of IRS proteins might result from increased protein stabilisation and were in agreement with the observed activation of Akt signalling in renal tumours of *Tsc2*^{+/-} mice.

Rapamycin attenuates activity of both Akt and mTORC1 in normal kidney tissues of *Tsc2*^{+/-} mice

Kidney tissues from 4 pairs of litter-mate $Tsc2^{+/-}$ mice treated for 6 weeks with rapamycin or vehicle were used for Western blot. Phosphorylation of Akt at S473 and its targets GSK3β at S9, eNOS at S1177 and MDM2 at S166 was reduced in kidney tissues of rapamycin treated mice compared to their vehicle treated litter mates (Figure 7). Phosphorylation of mTOR at S2448 and S2481, and S6 at S235/236 was also decreased in kidney tissues of rapamycin treated mice compared to their vehicle treated litter mates (Figure 7). Band shift in total 4EBP1 was observed indicating reduced phosphorylation in kidney tissues of rapamycin treated mice compared to their vehicle treated litter mates. No consistent increase or decrease in phosphorylation of Akt at T308 was detected in kidney tissues of rapamycin treated mice compared to their vehicle treated litter mates. Thus, rather than promoting Akt activity, rapamycin inhibited both Akt and mTORC1 in normal kidney tissues of $Tsc2^{+/-}$ mice.

Rapamycin effectively blocks tumourigenesis in the kidneys of $Tsc2^{+/-}$ mice by inhibiting Akt/mTOR signaling

To test whether rapamycin could prevent tumourigenesis in the kidneys of $Tsc2^{+/-}$ mice, we first established the earliest age at which renal lesions developed on the balb/c genetic background. We examined by microscopy H&E stained consecutive 5 μm kidney sections from 6 mice at each of the following ages: 15 days, 30 days, 45 days and 60 days. Only at 60 days of age were microscopic dysplastic lesions (RINs) seen together with microscopic cysts. We next randomly allocated litter-mate $Tsc2^{+/-}$ mice with balanced gender into two groups: rapamycin (n=20) and vehicle (n=20) (Supplemental Table 2). Treatment was commenced with rapamycin or vehicle at 1 month of age and continued until mice were sacrificed. Half of each group was sacrificed at 8 months and the remainder at 10 months. One mouse in the rapamycin treatment group died unexpectedly before the end of the experiment. No gross or microscopic renal lesions were found in this mouse but it was excluded from further analysis in this study. Analysis of renal pathology was carried out by a scientist and by a renal

pathologist both blinded to treatment status. Full coronal histological sections were taken at 200 µM intervals from every kidney. All macroscopically and microscopically observed lesions were counted, characterised and quantified by measuring both their maximum cross-sectional areas (lesion size) and also the areas representing only their cellular components, as described previously (30). The vehicle treated mice all had multiple bilateral renal lesions including RINs, cystic, papillary and solid lesions. By contrast, of 9 mice treated with rapamycin and sacrificed at 8 months only one showed 2 microscopic cysts (P < 0.0001) and no lesions were seen in any of 10 mice sacrificed at 10 months (P < 0.0001, Figure 8a; Supplemental Table 3). Thus rapamycin was highly effective in blocking tumourigenesis in the kidneys of $Tsc2^{+/-}$ mice.

We then examined the effect of long term treatment with rapamycin on Akt/mTOR signalling in the kidneys of $Tsc2^{+/-}$ mice. Kidney sections prepared from mice sacrificed at 10 months following treatment with rapamycin or vehicle were used for IHC. mTORC1 signalling appeared to be attenuated in rapamycin treated kidney tissues as indicated by reduced phosphorylation of S6 at S235/236 and 4EBP1 at S65 (Figure 8b). Akt signalling was also suppressed in rapamycin treated kidney tissues as indicated by reduced phosphorylation of Akt at S473 and its targets eNOS at S1177 and MDM2 at S166 although phosphorylation of Akt at T308 was variable in both rapamycin and vehicle treated tissues (Figure 8b).

DISCUSSION

We have investigated Akt/mTOR signalling in normal kidney tissues and renal lesions of a $Tsc2^{+/-}$ mouse model. We have demonstrated that feedback inhibition of Akt signalling appears to be lost in Tsc2-associated renal tumours that are characterised by activation of mTORC1. Our findings are unexpected because in MEF cells lacking either $Tsc1$ or $Tsc2$ Akt signalling is inhibited via a negative feedback loop elicited by activated mTOR/S6K

signalling (14, 15). Furthermore, based upon IHC-determined cytoplasmic and nuclear localization of FOXO1, feedback inhibition of Akt signalling was reported previously to be operating in liver hemangiomas in $Tsc2^{+/-}$ mice (21). Decreased phosphorylation of Akt at S473 detected by IHC has also indicated the existence of negative feedback on Akt signalling in human TSC-associated renal AMLs (31). In contrast, in $Tsc2^{+/-}$ mouse tumours, we found that FOXO1 was highly phosphorylated at S256, a specific Akt target site, and located in both the cytoplasm and the nucleus. Notably, we found that Akt was highly phosphorylated at S473 in all Tsc-associated tumours. Increased phosphorylation of multiple effectors of Akt was also observed in these tumours. To confirm these findings we used at least two different antibodies against each protein with two different IHC protocols (unpublished observations). Furthermore, the IHC data were entirely consistent with the findings of Western blot analyses.

Since Akt is specifically phosphorylated at T450 and S473 by mTORC2 (28, 29), our results suggested that mTORC2 was activated in $Tsc2^{+/-}$ mouse renal tumours. Consistent with this but in contrast to a previously published report (31), PKCα, another mTORC2 substrate (29), was also highly expressed and phosphorylated in the tumours. mTORC1 activation mediated feedback also suppresses MAPK activity in $Tsc2$ null cells and inhibition of mTORC1 induces MAPK pathway activation (32). However, we found that the MAPK pathway was activated in $Tsc2^{+/-}$ mouse renal lesions. Thus, multiple negative feedback loops mediated by mTORC1 activation that are well documented in $Tsc1$ or $Tsc2$ null MEFs may be disrupted in renal tumours of $Tsc2^{+/-}$ mice. The discrepancies between our findings and previous reports may reflect differences in tissue origins and types of Tsc-associated tumours in $Tsc2^{+/-}$ mice, as well as differences in mechanisms underlying tumourigenesis between human and mouse. The genetic background of mice studied may also contribute to

the differences. In the current study mice were maintained in a balb/c background while the $Tsc2^{+/-}$ mice used by others were crossed to a 129/SvJae background (21, 31). Future work should extend our study to a thorough investigation of Akt/mTOR signalling in different types of TSC-associated tumours in both human and mouse. Constitutively activated Akt might be required for initiation and progression of Tsc-associated renal tumours in $Tsc2^{+/-}$ mice. Indeed $Tsc1$ or $Tsc2$ null MEF cells with operational negative feedback of Akt signalling have reduced tumorigenic potential whereas following expression of myr-Akt or PDGFRβ these cells have increased Akt activity and exhibit accelerated tumour growth in nude mice (20). Phosphorylation of Akt at T308 and S473 is required for its full activation. PDK1 phosphorylates Akt at T308 and the Rictor-containing mTOR complex (mTORC2) phosphorylates Akt at S473. In this study, phosphorylation of Akt at T308 appeared to be variable in renal lesions of $Tsc2^{+/-}$ mice and this indicates that basal phosphorylation of this site might be sufficient for Akt activation in these tumours. Conditional complex gene knockouts ($Tsc2^{-/-}PDK1^{-/-}$ or $Tsc2^{-/-}Rictor^{-/-}$) in mouse kidneys may help to verify the role of Akt activation in Tsc-associated renal tumourigenesis.

mTORC1 activation appears to mediate feedback inhibition of PI3K/Akt signalling through multiple mechanisms in $Tsc1$ or $Tsc2$ null MEF cells (Figure 9). One mechanism is S6K directed transcriptional repression of $IRS1$ and phosphorylation of IRS proteins at multiple serine sites that induces degradation of IRS proteins (16, 17). Consistent with this notion, we found that both $Tsc2$ null MEFs and renal tumours showed suppressed transcription of $IRS1$ and $IRS2$ and increased serine phosphorylation of IRS proteins. Unexpectedly, both IRS1 and IRS2 protein levels were increased in renal lesions whereas $Tsc2$ null MEFs had marked reduction in expression of these proteins. This may partly explain the lost feedback inhibition seen in renal tumours. Recent studies have demonstrated

that mTORC1 exerts feedback inhibition of the PI3K and Erk-MAPK pathways through phosphorylation and stabilisation of Grb10 (18, 19). As expected, we found that *Tsc2* null MEFs showed increased protein levels and phosphorylation of Grb10 which were sensitive to rapamycin. By contrast, in renal tumours Grb10 protein levels appeared to be slightly reduced, although phosphorylation of at least one serine site was highly increased. It is possible that reduced Grb10 may contribute to the active Akt signalling we observed in these tumours. In some cultured cancer cells and tumour samples, mTORC1 inhibition abrogates feedback inhibition and activate PI3K/Akt signalling in an IGF1R dependent manner (33, 34). We found that IGF1R was consistently down regulated at transcriptional and protein levels in *Tsc2* null MEFs and in renal tumours of *Tsc2*$^{+/-}$ mice. Taken together, our results suggest that in *Tsc2*$^{+/-}$ mouse renal tumours mTORC1 activation-associated feedback loops may be disrupted due to changes in expression, phosphorylation or stability of multiple pathway components (Figure 9). Since IRS proteins have many candidate serine/threonine sites for phosphorylation, the patterns of phosphorylation of these proteins in *Tsc1* or *Tsc2* deficient tumours and MEF cells require further investigation in relation to the integrity of feedback loops. The ubiquitination machinery required for degradation of IRS proteins, for example cullin-RING E3 ubiquitin ligase 7 (35), should also be investigated in these tumours.

Rapamycin and its analogues have been used to treat various types of cancer and TSC–associated tumours in preclinical models and in humans (24-27). However, no properly designed study has been reported using rapamycin or its analogues for prevention of Tsc-associated renal tumours. This study provides the first proof of concept that Tsc-associated renal tumours are preventable by rapamycin. In addition to its inhibitory effects on mTORC1, prolonged treatment with rapamycin has been shown to inhibit Akt in tumour cells in a cell type dependent manner, and rapamycin-mediated inhibition of Akt may contribute to its

antitumor effect *in vivo* (36). While Akt signalling remains to be fully assessed in renal lesions of $Tsc2^{+/-}$ mice following rapamycin treatment, we have determined that long term treatment with rapamycin inhibits both mTORC1 and Akt in normal kidney tissues of $Tsc2^{+/-}$ mice. These results are consistent with previous findings by others that show an inhibitory effect of rapamycin on Akt in other normal tissues tested in wild type mice (37).

In conclusion, in contrast to previous studies, we have demonstrated that feedback inhibition of Akt signalling is lost in Tsc-associated renal lesions. Aberrant activation of both Akt and mTORC1 characterises Tsc-associated renal tumourigenesis in $Tsc2^{+/-}$ mice. By partially inhibiting the Akt/mTOR pathway, rapamycin appears sufficient to prevent Tsc-associated tumours. Our data suggest that clinical trials should assess whether tumour manifestations in patients with TSC are also amenable to prevention by rapamycin or its analogues. It is notable that the high dose of rapamycin used in the current study caused initial poor weight gain and later weight loss (Supplemental Figure 11). It will be important to establish whether lower doses are also effective before translation to clinical trials.

MATERIALS AND METHODS

Animal procedures

Animal procedures were performed in accordance with the UK Home Office guidelines and approved by the Ethical Review Group of Cardiff University. $Tsc2^{+/-}$ mice were described previously (22) and backcrossed to balb/c strain for over 10 times. Ear punches were used for DNA extraction and genotyping (22). For analysis of effect of rapamycin on molecular signalling in the kidneys by Western blot, 4 pairs of litter-mate $Tsc2^{+/-}$ mice (2 months old) were randomly allocated into two groups (rapamycin and vehicle) and treated for 6 weeks with 5 mg/kg rapamycin or vehicle 5 times a week. Rapamycin (LC Laboratories, Woburn,

13

USA) was prepared at 2 mg/ml in vehicle solution (2.5% PEG-400, 2.5% Tween-80 and 2.5% DMSO). These mice were humanely killed for tissue collection, and subsequent Western blot analysis. To test whether rapamycin could prevent renal tumourigenesis, 40 $Tsc2^{+/-}$ mice were randomly divided into 2 treatment groups: vehicle and rapamycin. All treatments were performed from the age of one month until sacrifice at 8 months or 10 months of age. Rapamycin was given by intra-peritoneal injection (i.p.) at 5 mg/kg 5 times a week initially but twice a week for the last 10 weeks due to concerns over weight loss. Rapamycin was given at 2.5 mg/kg once a week if rapid weight loss was observed. Mouse body weight was monitored once a week. At the end of treatment, animals were humanely killed for tissue collection, and subsequent histological and molecular analysis.

Cell Culture

Immortalised $TP53^{-/-}Tsc2^{+/+}$ and $TP53^{-/-}Tsc2^{-/-}$ MEF cells were described previously (38). Wild type and $Tsc1^{-/-}$ MEF cells were prepared directly from viable E11 litter mates wild type and $Tsc1^{-/-}$ embryos derived from inbreeding of a $Tsc1^{+/-}$ mouse model (23). Cells were routinely grown in either serum-free DMEM or DMEM (Life Technologies Ltd, Paisley, UK) containing 10% FBS, 50 units/ml penicillin and 50 µg/ml streptomycin at 37°C in a humidified 5% CO_2 incubator.

Histology

Assessment of mouse renal lesions was performed as described previously (30). Mouse kidneys were fixed in 10% buffered formalin saline (Thermo Scientific, Runcorn, UK) for 24 hours. Fixed kidneys were processed and paraffin-embedded according to standard procedures. A series of 5 µm coronal kidney sections were prepared with or without interruption at 200 µm intervals from each kidney. They were haematoxylin and eosin (HE) stained and scanned to create virtual HE slides using an Aperio system (http://www.aperio.com/?gclid=CNXN-8by4aUCFcINfAods3eg1w). Virtual slides were used

for lesion quantification. Maximum cross-sectional whole area and cellular area of each renal

lesion were measured respectively using ImageJ (http://rsbweb.nih.gov/ij). The assessment

was conducted blindly with respect to treatment status.

Immunohistochemistry (IHC)

Antibodies against phosphorylated 4EBP1 (4EBP1 p-T37/46, 4EBP1 p-S65, 4EBP1 p-T70),

Akt (pan), phosphorylated Akt (Akt p-T308, Akt p-S473, Akt p-T450), β-actin, GAPDH,

phosphorylated Grb10 (p-S476), phosphorylated GSK3α (GSK3α p-S21), phosphorylated

GSK3β (GSK3β p-S9), IRS1, phosphorylated IRS1 (p-S302), IRβ, IGF1Rβ, phosphorylated

Erk1/2 (p-T202/Y204), mTOR, S6, phosphorylated S6 (S6 p-S235/236), S6K and Tsc2 were

supplied by Cell Signalling Technology (Danvers, USA). Antibodies against Cyclin D1,

phosphorylated FOXO1A (FOXO1A p-S256), HIF1α, phosphorylated IRS2 (p-S731), Ki67

and MUC1 were supplied by abcam (Cambridge, UK). Antiboies against phosphorylated

eNOS (eNOS p-S1177), GLUT1, phosphorylated IKKα (IKKα p-T23), phosphorylated

MDM2 (MDM2 p-S166), phosphorylated mTOR (mTOR p-S2448, mTOR p-S2481),

phosphorylated RAF1 (RAF1 p-S259) and phosphorylated S6K (S6K p-T389) were supplied

by Sigma-Aldrich (Dorset, UK). Antibody against IRS2 was supplied by Insight

Biotechnology (Wembley, UK). Antibodies against Grb10 and phosphorylated Grb10 (p-

S501/503) were supplied by Millipore (U.K.) Limited (Watford, UK). XPOSE Rabbit

specific AP detection IHC kit (abcam, Cambridge, UK) or SignalStain Boost Rabbit specific

IHC Detection Reagent (Cell Signalling Technology, Danvers, USA) was used to stain

antigens. Briefly, paraffin-embedded mouse kidney sections were deparaffinised and

rehydrated. Sections were boiled for 10 minutes in 10 mM sodium citrate buffer (pH 6.0).

After cooling down in room temperature and 3 washes in TBST, sections were incubated in

1.5% goat serum for 10 minutes at room temperature. Antigen staining was performed

according to the kit supplier's instruction.

Western blot

Primary antibodies used for IHC were also used for Western blot. Additional antibodies were purchased for Western blot including those against Akt1, phosphorylated Akt1 (Akt1 p-S473), Akt2, Akt3, Erk1/2 and phosphorylated IGF1Rβ (p-Y1135/1136) (Cell Signalling Technology, Danvers, USA). Secondary antibody was horseradish peroxidise-conjugated antibody against rabbit (Cell Signalling Technology, Danvers, USA). Extracts of tumour samples, normal tissues or cultured cells were prepared using AllPrep DNA/RNA/Protein Mini Kit (QIAGEN Ltd-UK, Crawley, UK). Proteins were purified according to the kit supplier's instruction. Twenty µg of protein per sample was separated on NuPAGE 4-12% Bis-Tri**s** Gels **(**Life Technologies Ltd, Paisley, UK) and transferred onto Hybond ECL Membranes (GE Healthcare UK Ltd, Little Chalfont, UK). Blots were analysed with ECL Select Western Detection Kit (GE Healthcare UK Ltd, Little Chalfont, UK) and signals were detected using Autochemi Imaging System (UVP, Upland, USA).

Quantitative real time PCR (q-PCR)

Total RNA was isolated from mouse kidney tissues, renal tumours or cultured cells using AllPrep DNA/RNA/Protein Mini Kit and TissueRuptor (QIAGEN Ltd-UK, Crawley, UK). One microgram RNA was used to synthesise cDNA in a 20 µl solution using qScript cDNA SuperMix (Quanta BioSciences, Inc., Gaithersburg, USA). A PCR reaction containing 1 µl cDNA, 2 µl 2.5 µM primer mix, 6.5 µl 2xPerfecta SYBR SuperMix (Quanta BioSciences, Inc., Gaithersburg, USA) and 3.5 µl water was performed in a 7500 Real Time PCR System (Life Technologies Ltd**,** Paisley, UK). PCR was cycled as 95°C for 3 minutes, 40 cycles of 95°C for 15 seconds and 60°C for 1 minute. The relative quantification of target transcripts was obtained after normalisation to *HPRT*. Primer sequences for real time q-PCR were: GAGCTTCCTGTGAAAGTGATG and GATTCGGTTCTTCCAGGTC for *IGF1R*;

CGCTCCAGTGAGGATTTAAG and GGTCTTCATTCTGCTGTGATG for *IRS1*;

CTTCCTGTCCCATCACTTG and GTAGCGCTTCACTCTTTCAC for *IRS2* and

AGGGATTTGAATCACGTTTG and TTACTGGCAACATCAACAGG for *HPRT*.

Statistical Analysis

Fisher's exact test was used to compare lesion numbers between vehicle and rapamycin treated mice. Wilcoxon rank-sum (Mann-Whitney) test was performed to compare lesion size and lesion cellular areas between vehicle and rapamycin treated mice using the software Stata (version 11) (StataCorp LP, College Station, USA). $P < 0.05$ was considered to be statistically significant.

CONFLICT OF INTEREST

The authors declare no conflict of interest.

REFERENCES

1. Xu N, Lao Y, Zhang Y, Gillespie DA. Akt: a double-edged sword in cell proliferation and genome stability. *J Oncol* 2012; 2012: 951724.

2. Proud CG. mTOR Signalling in Health and Disease. *Biochem Soc Trans* 2011; 39: 431-436.

3. Russell RC, Fang C, Guan KL. An emerging role for TOR signalling in mammalian tissue and stem cell physiology. *Development* 2011; 138: 3343-3356.

4. Castedo M, Ferri KF, Kroemer G. Mammalian target of rapamycin (mTOR): pro- and anti-apoptotic. *Cell Death Differ* 2002; 9: 99-100.

5. Shaw RJ, Cantley LC. Ras, PI(3)K and mTOR signalling controls tumour cell growth. *Nature* 2006; 441: 424-430.

6. Guertin DA, Sabatini DM. Defining the role of mTOR in cancer. *Cancer Cell* 2007; 12: 9-22.

7. Dazert E, Hall MN. mTOR signalling in disease. *Curr Opin Cell Biol* 2011; 23: 744-755.

8. Song MS, Salmena L, Pandolfi PP. The functions and regulation of the PTEN tumour suppressor. *Nat Rev Mol Cell Biol* 2012; 13: 283-296.

9. Shaw RJ, Bardeesy N, Manning BD, Lopez L, Kosmatka M, DePinho RA *et al*. The LKB1 tumor suppressor negatively regulates mTOR signalling. *Cancer Cell* 2004; 6: 91-99.

10. Johannessen CM, Johnson BW, Williams SM, Chan AW, Reczek EE, Lynch RC *et al*. TORC1 is essential for NF1-associated malignancies. *Curr Biol* 2008; 18: 56-62.

11. Hasumi Y, Baba M, Ajima R, Hasumi H, Valera VA, Klein ME *et al.* Homozygous loss of BHD causes early embryonic lethality and kidney tumor development with activation of mTORC1 and mTORC2. *Proc Natl Acad Sci USA* 2009; 106: 18722-18727.

12. van Slegtenhorst M, de Hoogt R, Hermans C, Nellist M, Janssen B, Verhoef S *et al.* Identification of the tuberous sclerosis gene TSC1 on chromosome 9q34. *Science* 1997; 277: 805-808.

13. European Chromosome 16 Tuberous Sclerosis Consortium. Identification and characterization of the tuberous sclerosis gene on chromosome 16. *Cell* 1993; 75: 1305-1315.

14. Jaeschke A, Hartkamp J, Saitoh M, Roworth W, Nobukuni T, Hodges A *et al.* Tuberous sclerosis complex tumor suppressor-mediated S6 kinase inhibition by phosphatidylinositide-3-OH kinase is mTOR independent. *J Cell Biol* 2002; 159: 217-224.

15. Kwiatkowski DJ, Zhang H, Bandura JL, Heiberger KM, Glogauer M, el-Hashemite N *et al.* A mouse model of TSC1 reveals sex-dependent lethality from liver hemangiomas, and up-regulation of p70S6 kinase activity in Tsc1 null cells. *Hum Mol Genet* 2002; 11: 525-534.

16. Harrington LS, Findlay GM, Gray A, Tolkacheva T, Wigfield S, Rebholz H *et al.* The TSC1-2 tumor suppressor controls insulin-PI3K signalling via regulation of IRS proteins. *J Cell Biol* 2004; 166: 213-223.

17. Shah OJ, Wang Z, Hunter T. Inappropriate activation of the TSC/Rheb/mTOR/S6K cassette induces IRS1/2 depletion, insulin resistance, and cell survival deficiencies. *Curr Biol* 2004;14:1650-1656.

18. Yu Y, Yoon SO, Poulogiannis G, Yang Q, Ma XM, Villén J *et al.* Phosphoproteomic analysis identifies Grb10 as an mTORC1 substrate that negatively regulates insulin signalling. Science 2011; 332:1322-326

19. Hsu PP, Kang SA, Rameseder J, Zhang Y, Ottina KA, Lim D *et al.* The mTOR-regulated phosphoproteome reveals a mechanism of mTORC1-mediated inhibition of growth factor signalling. Science 2011; 332:1317-1322.

20. Zhang H, Bajraszewski N, Wu E, Wang H, Moseman AP, Dabora SL *et al.* PDGFRs are critical for PI3K/Akt activation and negatively regulated by mTOR. *J Clin Invest* 2007; 117: 730-738.

21. Manning BD, Logsdon MN, Lipovsky AI, Abbott D, Kwiatkowski DJ, Cantley LC. Feedback inhibition of Akt signalling limits the growth of tumors lacking Tsc2. *Genes Dev* 2005; 19:1773-1778.

22. Onda H, Lueck A, Marks PW, Warren HB Kwiatkowski DJ. Tsc2(+/-) mice develop tumors in multiple sites that express gelsolin and are influenced by genetic background. *J Clin Invest* 1999; 104: 687-695.

23. Wilson C, Idziaszczyk S, Parry L, Guy C, Griffiths DF, Lazda E *et al.* A mouse model of tuberous sclerosis 1 showing background specific early post-natal mortality and metastatic renal cell carcinoma. *Hum Mol Genet* 2005; 14: 1839-1850.

24. Lee L, Sudentas P, Donohue B, Asrican K, Worku A, Walker V *et al.* Efficacy of a rapamycin analog (CCI-779) and IFN-gamma in tuberous sclerosis mouse models. *Genes Chromosomes Cancer* 2005; 42: 213-227.

25. Pollizzi K, Malinowska-Kolodziej I, Stumm M, Lane H, Kwiatkowski D. Equivalent benefit of mTORC1 blockade and combined PI3K-mTOR blockade in a mouse model of tuberous sclerosis. *Mol Cancer* 2009; 8: 38.

26. Bissler JJ, McCormack FX, Young LR, Elwing JM, Chuck G, Leonard JM *et al.* Sirolimus for angiomyolipoma in tuberous sclerosis complex or lymphangioleiomyomatosis. *N Engl J Med* 2008; 358: 140-151.

27. Krueger DA, Care MM, Holland K, Agricola K, Tudor C, Mangeshkar P *et al.* Everolimus for subependymal giant-cell astrocytomas in tuberous sclerosis. *N Engl J Med* 2010; 363: 1801-1811.

28. Guertin DA, Stevens DM, Thoreen CC, Burds AA, Kalaany NY, Moffat J *et al.* Ablation in mice of the mTORC components raptor, rictor, or mLST8 reveals that mTORC2 is required for signalling to Akt-FOXO and PKCalpha, but not S6K1. *Dev Cell* 2006;11:859-871.

29. Ikenoue T, Inoki K, Yang Q, Zhou X, Guan KL. Essential function of TORC2 in PKC and Akt turn motif phosphorylation, maturation and signalling. *EMBO J* 2008; 27:1919-1931

30. Kalogerou M, Zhang Y, Yang J, Garrahan N, Paisey S, Tokarczuk P *et al.* T2 weighted MRI for assessing renal lesions in transgenic mouse models of tuberous sclerosis. *Eur J Radiol* 2012; 81: 2069-2074.

31. Huang J, Wu S, Wu CL, Manning BD. Signaling events downstream of mammalian target of rapamycin complex 2 are attenuated in cells and tumors deficient for the tuberous sclerosis complex tumor suppressors. *Cancer Res* 2009; 69: 6107-6114.

32. Carracedo A, Ma L, Teruya-Feldstein J, Rojo F, Salmena L, Alimonti A *et al.* Inhibition of mTORC1 leads to MAPK pathway activation through a PI3K-dependent feedback loop in human cancer. *J Clin Invest* 2008; 118: 3065-3074.

33. O'Reilly KE, Rojo F, She QB, Solit D, Mills GB, Smith D *et al.* mTOR inhibition induces upstream receptor tyrosine kinase signalling and activates Akt. *Cancer Res* 2006; 66: 1500-1508.

34. Wan X, Harkavy B, Shen N, Grohar P, Helman LJ. Rapamycin induces feedback activation of Akt signalling through an IGF-1R-dependent mechanism. *Oncogene* 2007; 26: 1932-1940.

35. Xu X, Keshwani M, Meyer K, Sarikas A, Taylor S, Pan ZQ. Identification of the degradation determinants of insulin receptor substrate 1 for signaling cullin-RING E3 ubiquitin ligase 7-mediated ubiquitination. *J Biol Chem* 2012; 287: 40758-66.

36. Sarbassov DD, Ali SM, Sengupta S, Sheen JH, Hsu PP, Bagley AF *et al.* Prolonged rapamycin treatment inhibits mTORC2 assembly and Akt/PKB. *Mol Cell* 2006; 22: 159-168.

37. Lamming DW, Ye L, Katajisto P, Goncalves MD, Saitoh M, Stevens DM *et al.* Rapamycin-induced insulin resistance is mediated by mTORC2 loss and uncoupled from longevity. *Science* 2012; 335: 1638-1643.

38. Zhang H, Cicchetti G, Onda H, Koon HB, Asrican K, Bajraszewski N *et al.* Loss of Tsc1/Tsc2 activates mTOR and disrupts PI3K-Akt signalling through downregulation of PDGFR. *J Clin Invest* 2003; 112: 1223-1233.

Figure Legends

Figure 1 Analysis of Tsc2 expression in renal tumours of *Tsc2*^{+/-} mice

Kidney sections from *Tsc2*^{+/-} mice of 10 months old were prepared and stained by IHC with an antibody against Tsc2. Representative kidney sections were presented showing lack of Tsc2 expression (**a**), reduced Tsc2 expression (**b**) and expression of Tsc2 (**c**) in renal lesions. Scale bars are 100.1 µm.

Figure 2 mTOR signalling in kidney tissues and tumours of *Tsc2*^{+/-} mice

a. *Tsc2*^{+/-} mice were sacrificed at 10 months of age. Kidney sections were prepared and stained with antibodies against total and phosphorylated mTOR at S2448 and S2481 by IHC. Scale bars are 100 µm.

b. *Tsc2*^{+/-} mice were sacrificed at 10 months of age. Kidney sections were prepared and stained with antibodies against mTOR targets by IHC: total and phosphorylated S6K at T389, S6 at S235/236, and 4EBP1 at S65 and T37/46/70. Scale bars are100 µm.

c. *Tsc2*^{+/-} mice were sacrificed at 10 months of age. Proteins were prepared from paired normal kidney tissues (N) and kidney tumours (T) of the same mice, and used for Western blot to analyse expression of total mTOR, S6K, S6, and phosphorylation of mTOR at S2448 and S2481, S6K at T389, S6 at S235/236, and 4EBP1 at S65 and T37/46. Genotyping for *Tsc2* by PCR and expression analysis of Tsc2 by Western blot in kidney and tumour cells were shown in the bottom panel.

Figure 3 Akt signalling in kidney tissues and tumours of *Tsc2*$^{+/-}$ mice

a. *Tsc2*$^{+/-}$ mice were sacrificed at 10 months of age. Kidney sections were prepared and stained with antibodies against total and phosphorylated Akt at T308, T450 and S473 by IHC. Scale bars for whole kidney sections are 5 mm and for the rest 100 µm.

b. *Tsc2*$^{+/-}$ mice were sacrificed at 10 months of age. Kidney sections were prepared and stained with antibodies against Akt targets by IHC: total HIF1α and GLUT1, and phosphorylated eNOS, MDM2, GSK3α, GSK3β, IKKα and RAF1. Scale bars are 100 µm.

c. *Tsc2*$^{+/-}$ mice were sacrificed at 10 months of age. Proteins were prepared from paired normal kidney tissues (N) and kidney tumours (T) of the same mice, and used for Western blot to analyse expression of total Akt, Akt1, Akt2 and Akt3, and phosphorylation of Akt at s473, T450 and T308, Akt1 at s473, eNOS at s1177, MDM2 at s166, GSK3α at s21 and GSK3β at s9. Genotyping for *Tsc2* by PCR and expression analysis of Tsc2 by Western blot in kidney and tumour cells were shown in the bottom panel.

Figure 4 PKCα signalling in kidney tissues and tumours of *Tsc2*$^{+/-}$ mice

a. *Tsc2*$^{+/-}$ mice were sacrificed at 10 months of age. Kidney sections were prepared and stained with antibodies against total and phosphorylated PKCα at T638 and S657 by IHC. Scale bars 100 µm.

b. *Tsc2*$^{+/-}$ mice were sacrificed at 10 months of age. Proteins were prepared from paired normal kidney tissues (N) and kidney tumours (T) of the same mice, and used for Western blot to analyse expression of total and phosphorylated PKCα at T638 and S657. Genotyping for *Tsc2* by PCR and expression analysis of Tsc2 by Western blot in kidney and tumour cells were shown in the bottom panel.

Figure 5 Comparison of mTOR/Akt feedback signalling between renal tumours of _Tsc2_$^{+/-}$ mice and cultured _Tsc2_$^{-/-}$ MEF cells

Tsc2$^{+/-}$ mice were sacrificed at 10 months of age. Proteins were prepared from paired normal kidney tissues (N) and kidney tumours (T) of the same mice (left panel). Proteins were also prepared from immortalised _TP53_$^{-/-}$_Tsc2_$^{+/+}$ or _TP53_$^{-/-}$_Tsc2_$^{-/-}$ MEF cells which were grown in serum free DMEM for 16 hours (right panel). Proteins were then used for Western blot to analyse expression of total IRS1, IRS2, Grb10, IRβ, IGF1Rβ, Erk1/2, and GAPDH, and phosphorylation of IRS1 at S302, IRS2 at S731, Grb10 at S476 and S501/503, IGF1Rβ at Y1135/1136, Erk1/2 at T202/Y204, Akt at S473 and S6 at S235/236.

Figure 6 Analysis of expression and phosphorylation of IRS and Grb10 proteins in renal tumours of _Tsc2_$^{+/-}$ mice

Tsc2$^{+/-}$ mice were sacrificed at 10 months of age. Kidney sections were prepared and stained by IHC with antibodies against total IRβ, IGF1Rβ, IRS1, IRS2 and Grb10, and phosphorylated IRS1 at S302, IRS2 at S731 and Grb10 at S476. Scale bars are 100 µm.

Figure 7 Inhibition of Akt/mTOR signalling by rapamycin in kidney tissues of _Tsc2_$^{+/-}$ mice

Four pairs of litter-mate _Tsc2_$^{+/-}$ mice were randomly allocated into two groups and treated for 6 weeks with 5 mg/kg rapamycin or vehicle 5 times a week. Mice were sacrificed and one kidney each mouse was used for protein preparation and Western blot. Western blots were probed with antibodies against phosphorylated Akt at T308 and S473, GSK3β at S9, eNOS at S1177, MDM2 at S166, mTOR at S2448 and S2481, and S6 at S235/236, and total 4EBP1.

Figure 8 Prevention of renal tumourigenesis by inhibition of Akt/mTOR signalling with rapamycin in _Tsc2_$^{+/-}$ mice

a. Prevention of renal tumourigenesis. *Tsc2*^{+/-} mice were treated from one month old until sacrifice at the age of 8 months (top panel) (vehicle, n=10; rapamycin, n=9) or 10 months (bottom panel) (vehicle, n=10; rapamycin, n=10). Dosages are described in Methods. Kidney sections were prepared for histological assessment of treatment effect. Lesion number and size (area) as well as lesion cellular area were compared for mice sacrificed at the age of 8 and 10 months respectively. Horizontal bars indicate a median. All the mice treated with vehicle developed multiple lesions at both ages. In contrast, only two microscopic cysts were seen in one of the rapamycin treated mice at the age of 8 months. For detailed statistical analysis see Supplemental Table 3.

b. Inhibition of Akt/mTOR signalling. *Tsc2*^{+/-} mice were treated as described above. Kidney sections were prepared for IHC analysis using antibodies against phosphorylated S6 at S235/236, 4EBP1 at S65, Akt at T308 and S473, eNOS at S1177 and MDM2 at S166.

Figure 9 Model for loss of feedback inhibition of PI3K/Akt and Ras/Erk signaling in *Tsc1*^{-/-} or *Tsc2*^{-/-} renal tumour cells

On the left is a representation of a MEF cell lacking functional Tsc1 or Tsc2.This shows mTORC1 activation-mediated feedback inhibition of PI3K/Akt and Ras/Erk signalling through multiple mechanisms including serine phosphorylation of IRS proteins by mTOR/S6K1 and their subsequent degradation. Solid red lines show feedback via established mechanisms; broken red lines show feedback where precise mechanisms remain to be determined. Activated pathway components are shown in dark green and inhibited components in grey. On the right is a representation of a *Tsc1*^{-/-} or *Tsc2*^{-/-} renal tumour cell. "X" indicates possibly disrupted feedback loops. The activation status of pathway components in light green requires further study as do their relationships (broken black lines). Additional genetic and epigenetic changes may contribute to disruption of feedback

loops in tumour cells, leading to stabilisation of IRS proteins, increased Akt activity and Erk activation.
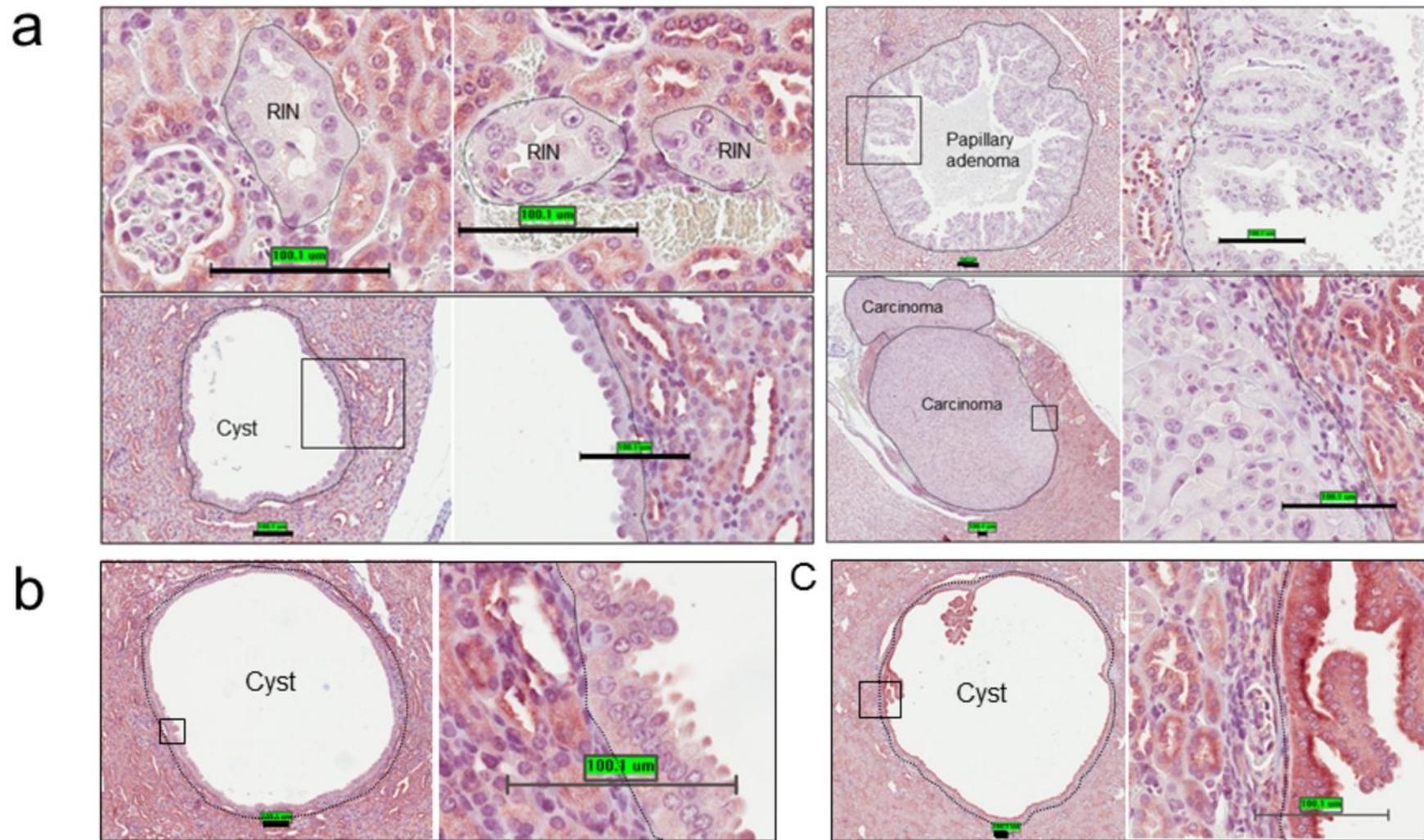
Figure 1
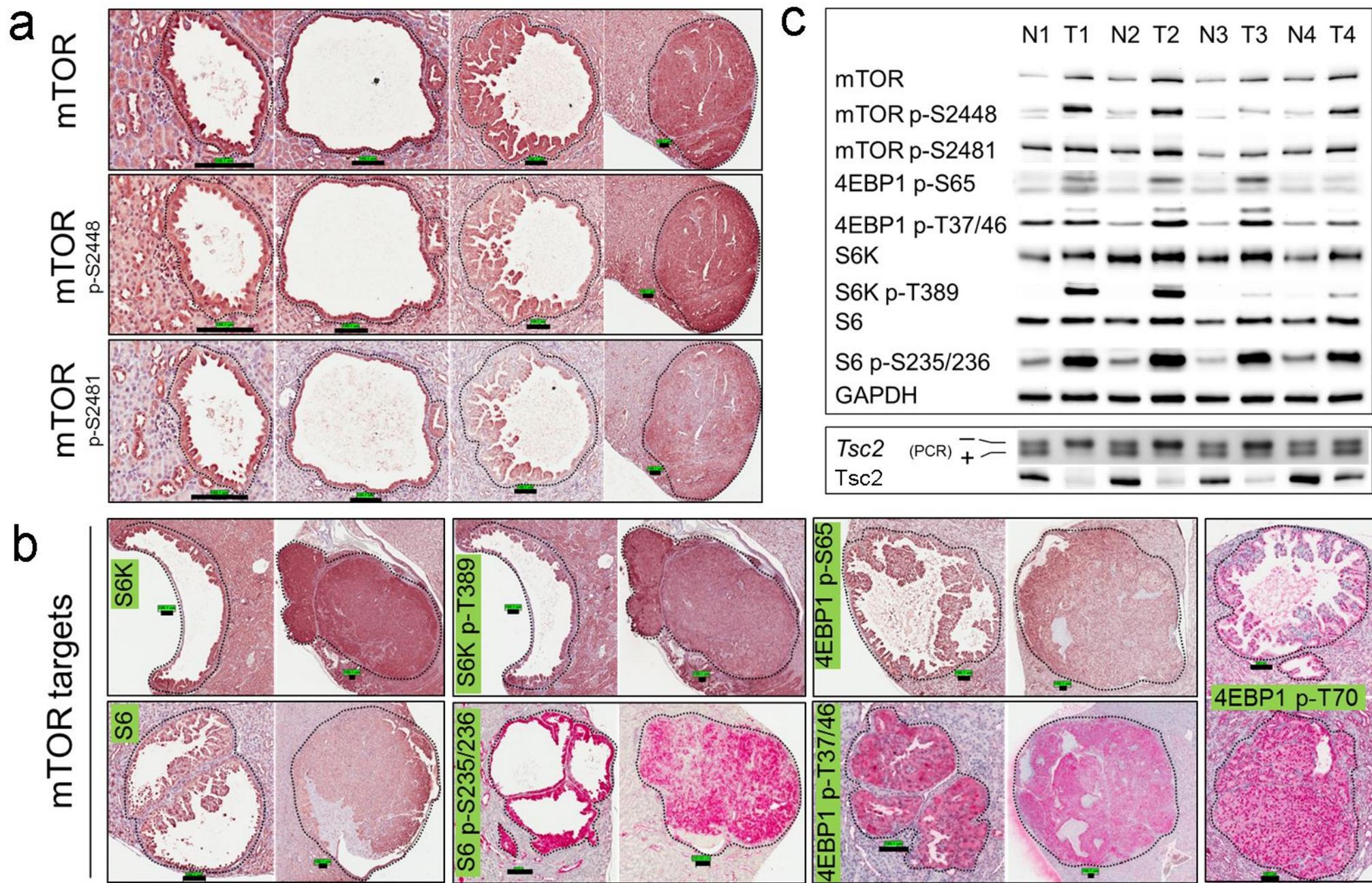
Figure 2
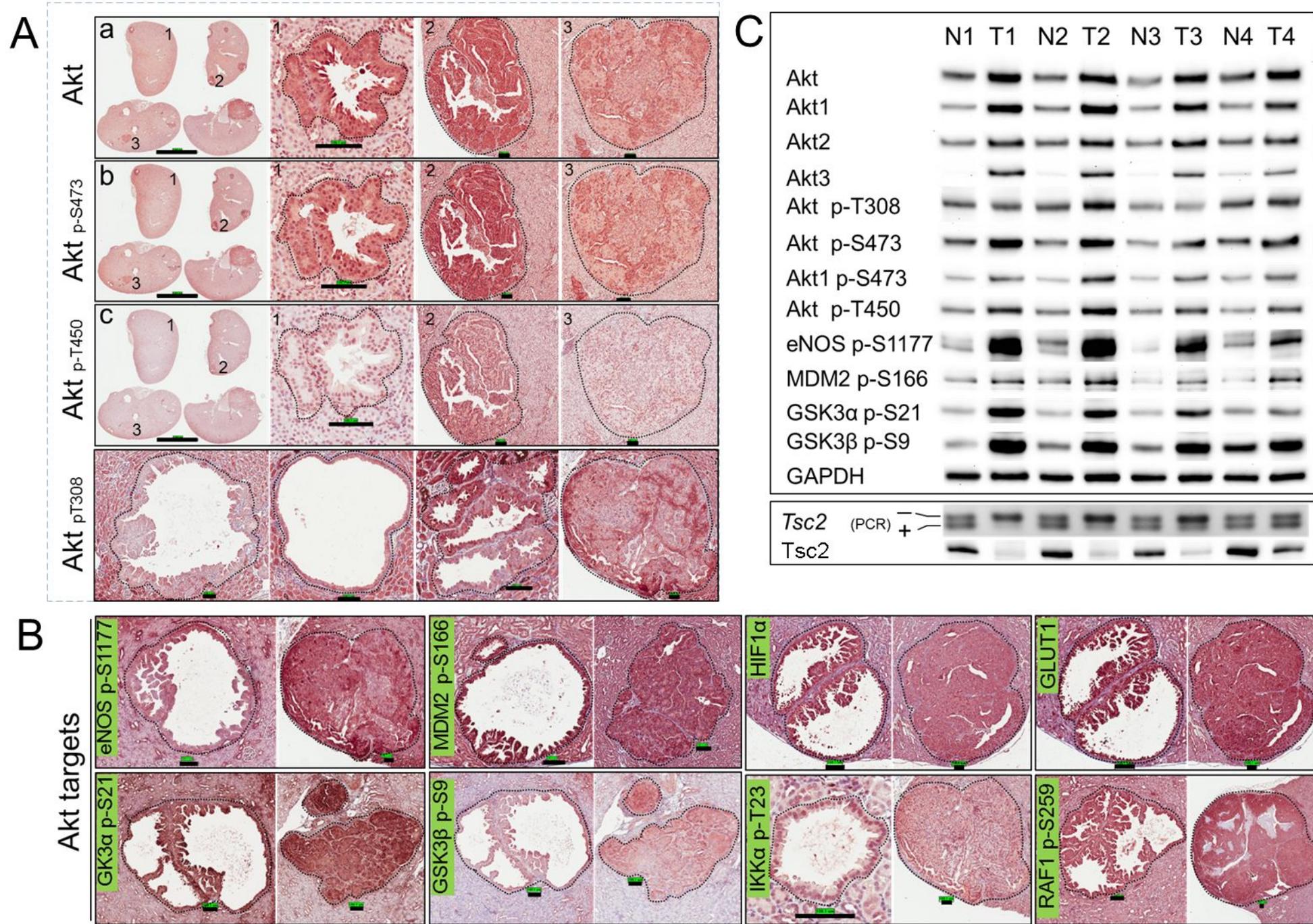
Figure 3
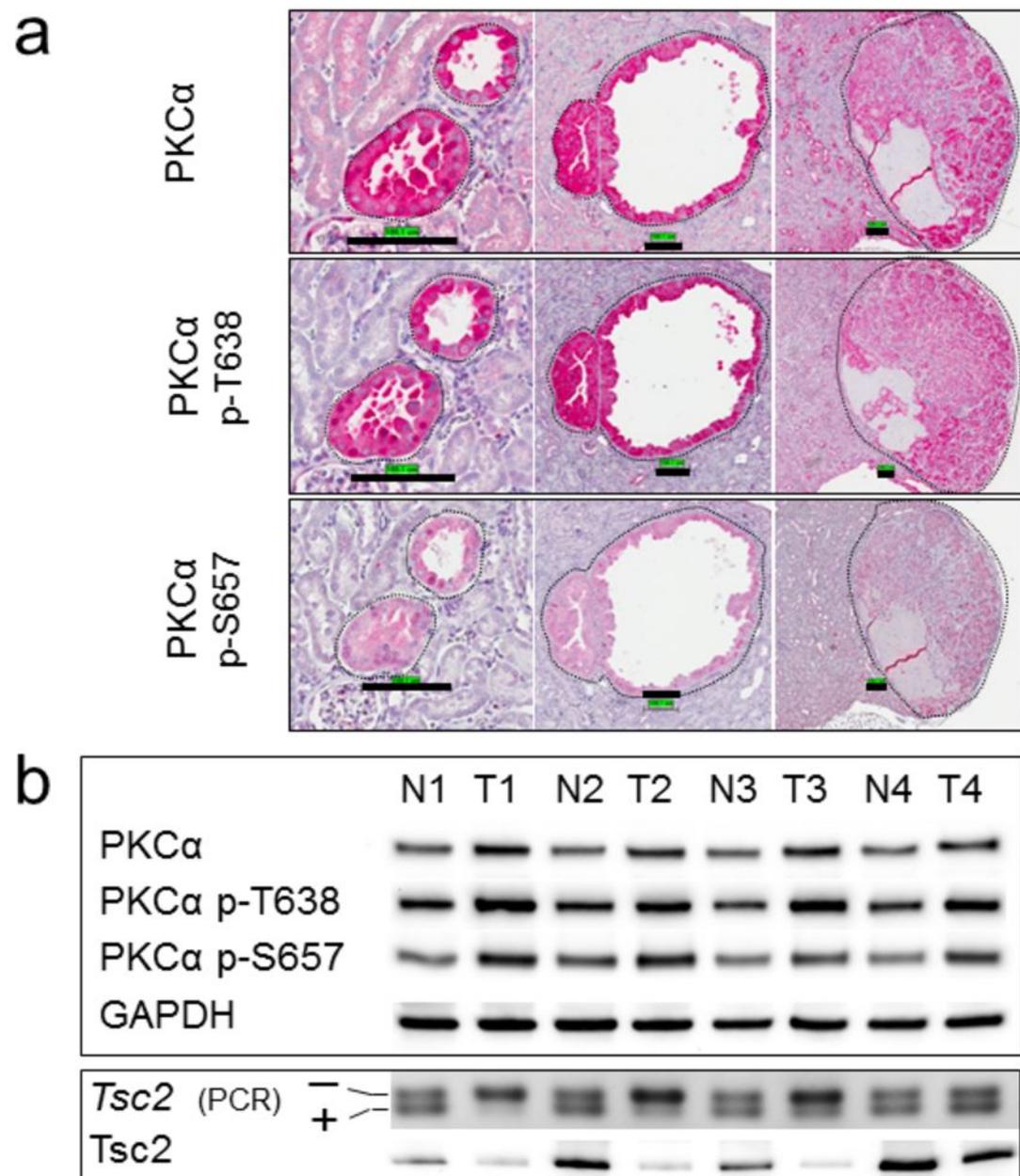
Figure 4

Mouse kidney and tumour samples — N1 T1 N2 T2 N3 T3 N4 T4

MEF cells — *Tsc2* +/+ -/-

IRS1
IRS1 p-S302
IRS2
IRS2 p-S731
Grb10
Grb10 p-S476
Grb10 p-S501/503
IRβ
IGF1Rβ
IGF1Rβ p-Y1135/1136
Erk1/2
Erk1/2 p-T202/Y204
Akt p-S473
S6 p-S235/236
GAPDH
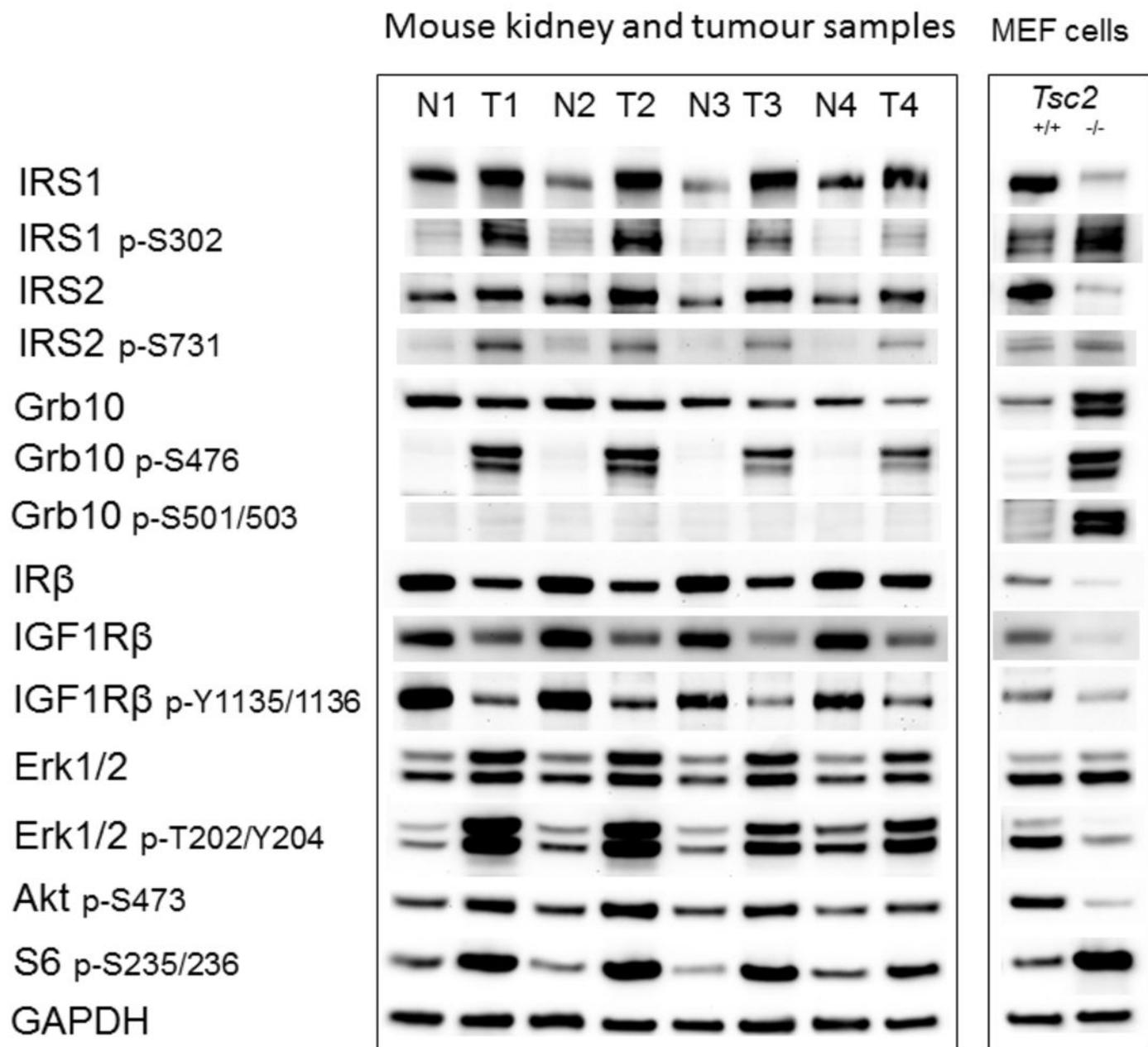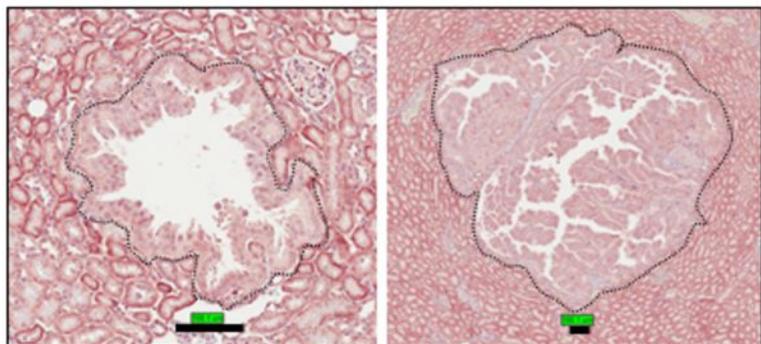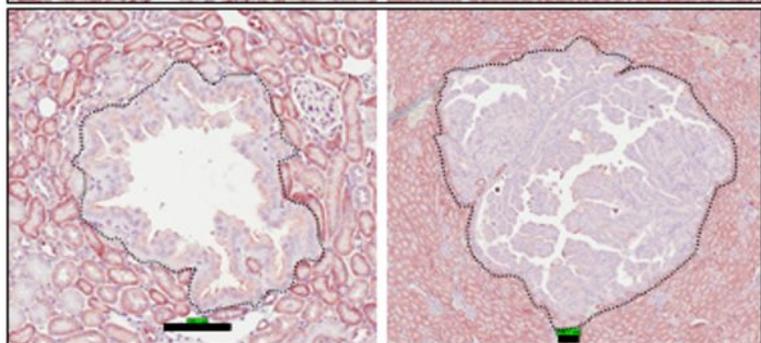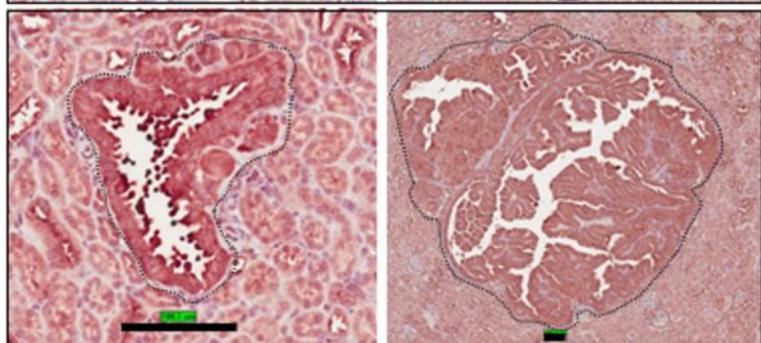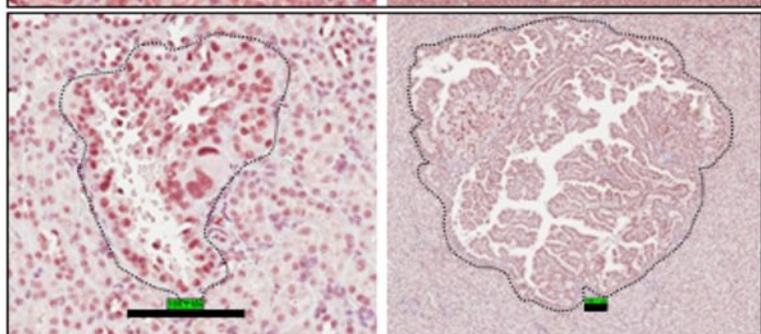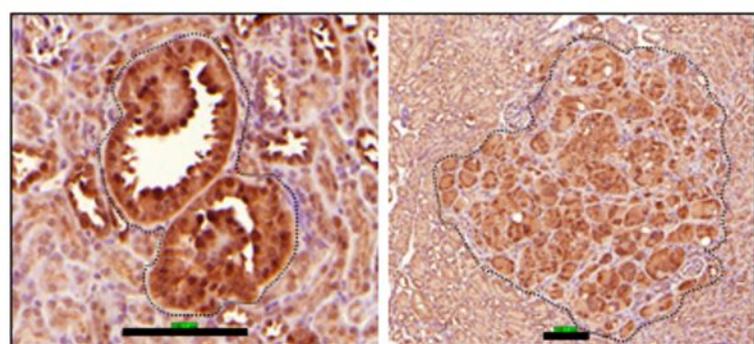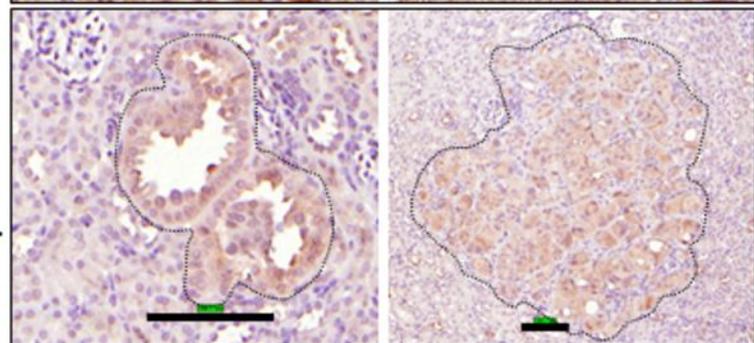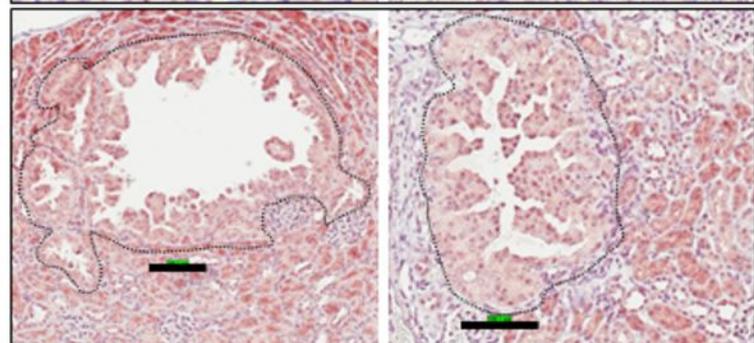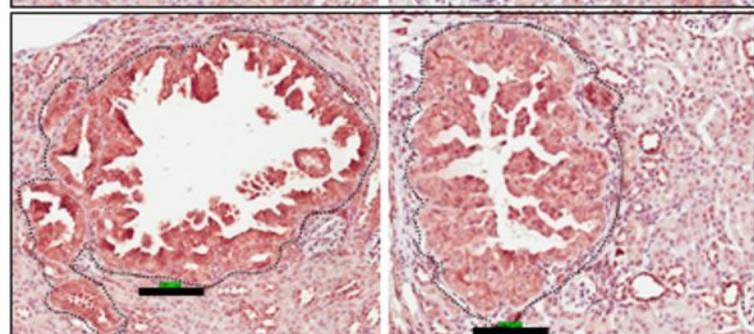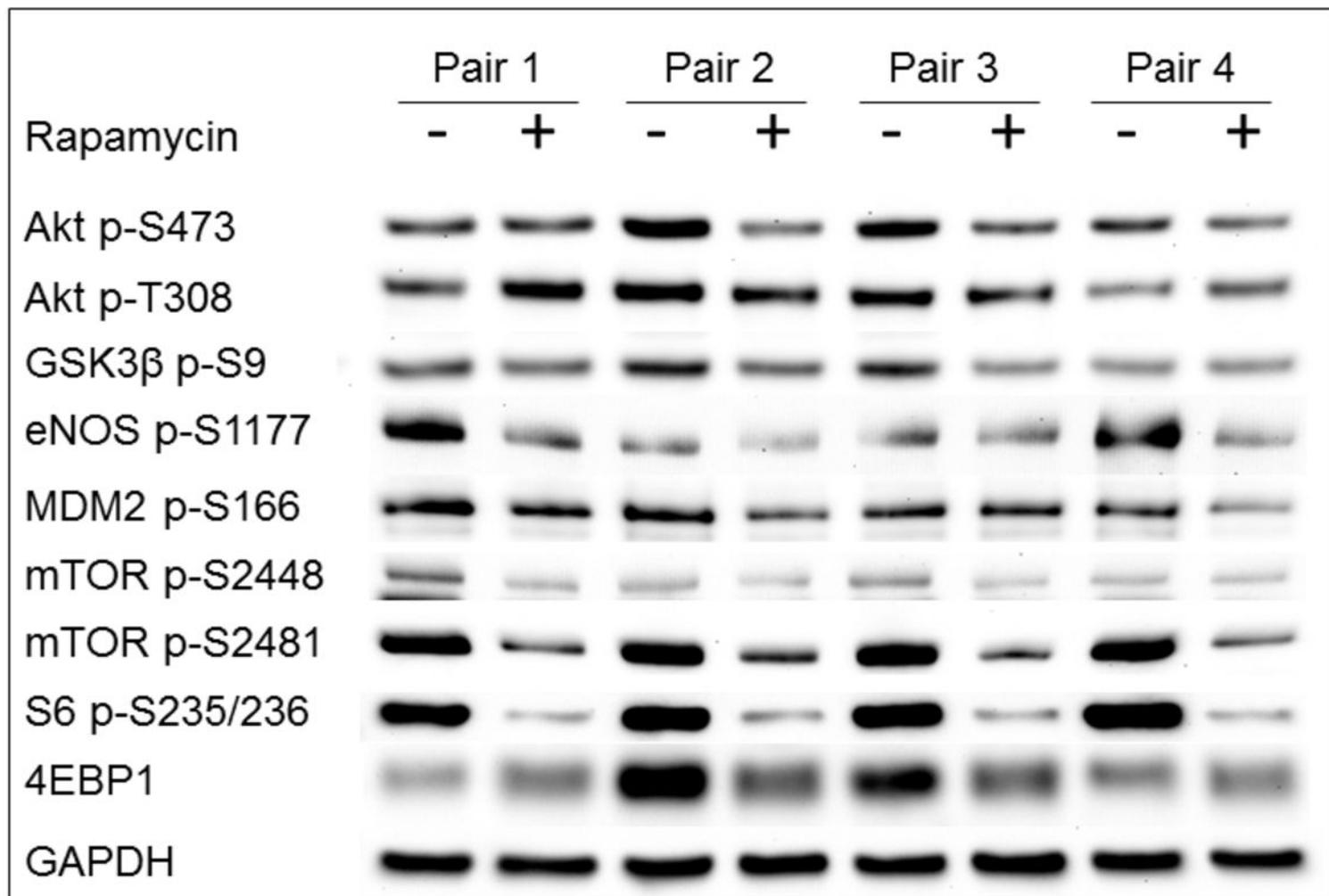
Figure 5

Figure 6

Figure7

Figure 8

Figure 9